Short report

Biallelic *GINS2* variant p.(Arg114Leu) causes Meier-Gorlin syndrome with craniosynostosis

Maria J Nabais Sá ,[1,2] Kerry A Miller,[3] Mary McQuaid,[4] Nils Koelling,[3] Andrew O M Wilkie ,[3] Hugo Wurtele,[4] Arjan P M de Brouwer,[1] Jorge Oliveira [5,6]

► Additional supplemental material is published online only. To view, please visit the journal online (http://dx.doi.org/10.1136/jmedgenet-2020-107572).

For numbered affiliations see end of article.

Correspondence to
Dr Maria J Nabais Sá, Department of Human Genetics (route 836), Radboud University Medical Center, P.O. box 9101, 6500 HB, Nijmegen, The Netherlands; maria.nabaissa@gmail.com

MJNS and KAM contributed equally.

Received 5 November 2020
Accepted 14 July 2021
Published Online First 5 August 2021

To cite: Nabais Sá MJ, Miller KA, McQuaid M, *et al*. *J Med Genet* 2022;**59**:776–780.

ABSTRACT

Introduction Replication of the nuclear genome is an essential step for cell division. Pathogenic variants in genes coding for highly conserved components of the DNA replication machinery cause Meier-Gorlin syndrome (MGORS).

Objective Identification of novel genes associated with MGORS.

Methods Exome sequencing was performed to investigate the genotype of an individual presenting with prenatal and postnatal growth restriction, a craniofacial gestalt of MGORS and coronal craniosynostosis. The analysis of the candidate variants employed bioinformatic tools, *in silico* structural protein analysis and modelling in budding yeast.

Results A novel homozygous missense variant NM_016095.2:c.341G>T, p.(Arg114Leu), in *GINS2* was identified. Both non-consanguineous healthy parents carried this variant. Bioinformatic analysis supports its classification as pathogenic. Functional analyses using yeast showed that this variant increases sensitivity to nicotinamide, a compound that interferes with DNA replication processes. The phylogenetically highly conserved residue p.Arg114 localises at the docking site of CDC45 and MCM5 at GINS2. Moreover, the missense change possibly disrupts the effective interaction between the GINS complex and CDC45, which is necessary for the CMG helicase complex (Cdc45/MCM2–7/GINS) to accurately operate. Interestingly, our patient's phenotype is strikingly similar to the phenotype of patients with *CDC45*-related MGORS, particularly those with craniosynostosis, mild short stature and patellar hypoplasia.

Conclusion *GINS2* is a new disease-associated gene, expanding the genetic aetiology of MGORS.

INTRODUCTION

Meier-Gorlin syndrome (MGORS) is characterised by a triad of clinical findings consisting of: (1) prenatal and postnatal growth retardation, (2) microtia, and (3) absent or hypoplastic patellae.[1] This disorder is caused by pathogenic variants in genes coding for evolutionarily conserved components of the replication machinery of the nuclear genome—*ORC1*, *ORC4*, *ORC6*, *CDT1*, *CDC6*, *GMNN*, *CDC45*, *MCM5* and *DONSON*.[2–7] Six ORC proteins (ORC1–6), Cdc6, Cdt1 and a heterohexamer of MCM proteins (MCM2–7) form a prereplication complex, which is activated by binding of Cdc45 and the heterotetramer GINS (GINS1–4) to MCM2–7.[8] The resultant preinitiation CMG complex (Cdc45/MCM2–7/GINS) is a DNA helicase that separates the two strands of the DNA double helix at replication origins, subsequently enabling their replication.[8]

The genotype of individuals with MGORS requires at least one allele of genes encoding essential DNA replication factors allowing for some residual activity (hypomorphic variant).[2–6] Furthermore, less severe phenotypes are often associated with two hypomorphic variants, while more severe phenotypes result from a combination of a hypomorphic and a loss-of-function variant.[1] Nevertheless, in approximately 20% of individuals no pathogenic variants have been detected.[1] Here, we describe the first patient with a homozygous disease-causing variant in *GINS2*, a subunit of the preinitiation CMG helicase, presenting with craniosynostosis and fulfilling the clinical diagnosis of MGORS.

METHODS

The family was enrolled with informed consent into the Genetics Basis of Craniofacial Malformations study. The individual's phenotype was longitudinally and systematically evaluated. Exome capture, sequencing and analysis of DNA extracted from peripheral blood cells of the proband and both parents were carried out as described in online supplemental methods. We analysed the data assuming complete penetrance, allowing for the possibility of either a *de novo* variant (dominant) or biallelic inheritance (recessive). *In silico* protein analysis of CMG structures was performed for mutation prediction over stability and interactions, as detailed in online supplemental methods. One patient variant was further characterised using budding yeast *Saccharomyces cerevisiae*, as described in online supplemental methods, online supplemental table 5, online supplemental table 6.

RESULTS

A 2-month-old girl was referred for genetic evaluation due to intrauterine growth restriction (IUGR), short stature, microcephaly and facial dysmorphisms. She was the only child of a non-consanguineous healthy Portuguese couple with an unremarkable family history. During pregnancy, IUGR was diagnosed at the 29th week of gestation. Fetal structural abnormalities, infections and teratogens were excluded. She was born at 37^{+5} gestational weeks, by eutocic delivery with Apgar scores 9 and 10, at first and fifth minutes. At birth, her

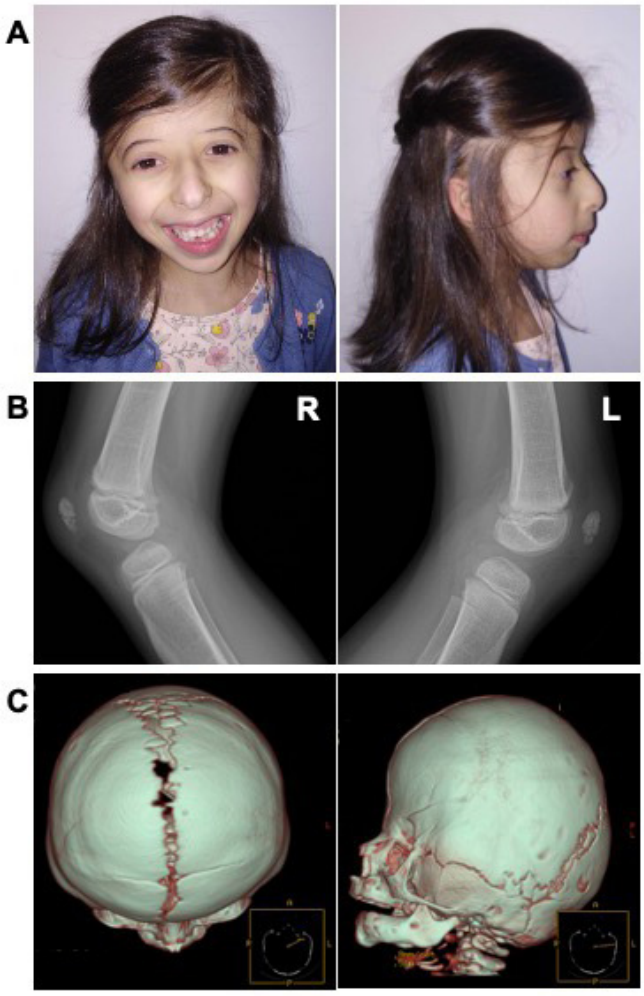

Figure 1 Clinical findings of an individual with a homozygous missense *GINS2* variant. (A) Craniofacial features of Meier-Gorlin syndrome at 6 years of age, including microtia, thin eyebrows, a narrow nose with a convex nasal ridge, microstomia, full lips and microretrognathia. (B) Lateral radiographic view of both knees at 7 years of age, showing hypoplastic patellae. (C) 3D reconstruction of cranial CT scans at 5 months old, demonstrating an incomplete premature fusion of coronal sutures. L, left knee; R, right knee.

weight was 2260 g (1st centile; −2.2 SD), her length was 47 cm (~10th centile) and her head circumference (HC) was 30.5 cm (<1st centile; −3 SD). She had neonatal jaundice and mild hypotonia. Poor suction and feeding difficulties were noticed and gastro-oesophageal reflux was diagnosed. Newborn metabolic screening was normal. Newborn hearing screening failed, but auditory-evoked potentials at age of 10 days were within the normal electrophysiological limits.

She presented with craniofacial dysmorphic features, which evolved with age (figure 1). Her head was microcephalic and brachycephalic and her neck was short. At 6 months, her face was round with a narrow forehead and a low hairline, mid-face hypoplasia and microretrognathia. Ears were small, low set and posteriorly rotated with an atretic external auditory canal. Eyes were prominent and palpebral fissures were downslanted. Her nose was short with a wide, depressed nasal bridge, a convex nasal ridge, hypoplastic nares, low insertion of the columella and long philtrum. Her mouth was small with downturned corners, full lips and a high narrowed palate. She also had short and tapering fingers, short toes, a sacral dimple, an anteriorly placed anus and hypopigmented macules on the abdomen and upper back. At 6 years of age, hypopigmented macules were also observed on the arms and legs.

A bilateral coronal craniosynostosis was confirmed by cranial CT performed at 5 months old (figure 1), and surgically corrected at 17 months. Delayed teeth eruption was observed, with the first tooth erupting after 16 months of age. Her height, weight and HC improved with age (online supplemental table 1). Psychomotor development was adequate. During childhood, she had recurrent respiratory infections.

Extensive system-based investigation was performed. Left ureteropelvic ectasia was noticed during an abdominal and renovesical ultrasound at 16 days. During the cardiological examination at 1 month of age, a patent foramen ovale and an atrial septal defect (ASD) of 5 mm with a left-right shunt were diagnosed. At 15 months, no ECG abnormalities were observed. Surgical closure of the ASD took place at 5 years and 9 months old. Four months before this surgery, she had an *ostium secundum*-type ASD of about 10 mm and a sinus venous-type ASD of about 5 mm, resulting in a left-right shunt and dilated right cavities. A mild tricuspid regurgitation with a right ventricle/right auricle gradient of about 16 mm Hg had also been detected. A complete skeletal X-ray at 21 months did not show skeletal abnormalities. Left wrist X-ray at 22 months demonstrated delayed bone age (10–12 months). Ophthalmological evaluation at 22 months diagnosed myopia. Lymphocyte immunophenotyping study at 2 years and 10 months did not show quantitative changes suggestive of any immunodeficiency. Finally, knee radiography, performed at 7 years of age, showed hypoplastic patellae (figure 1).

Given prenatal and postnatal growth delay, bilateral coronal craniosynostosis, cardiac defects and craniofacial dysmorphic features, standard diagnostic genetic investigation was performed. Karyotype, chromosomal microarray and direct sequencing of the *FGFR2*, *FGFR3* (exons 7 and 10) and *TWIST* did not identify pathogenic variants. Through exome sequencing, a homozygous missense variant NM_016095.2:c.341G>T, p.(Arg114Leu), was identified in the *GINS2* gene (MIM*610609) as the most likely candidate genetic cause of the observed primordial dwarfism and craniosynostosis phenotype. Other variants in candidate genes (online supplemental table 2) were excluded from further experimental studies. The single heterozygous variant in *UBQLN3* gene was reported in gnomAD at a low frequency (two heterozygotes listed in this database). As for the compound heterozygous variants identified in four different genes, they were also underrated considering: (1) the lower deleterious score or inconsistency between bioinformatic predictors (*ANKRD11*, *RIF1* and *SYNJ2*); and (2) the protein's known biological function did not correlate with the patient's phenotype (*AHNAK*). The cumulative size of all runs of homozygosity (ROH) was estimated at 18.6 Mb, representing <1% of the genome and excluding any close consanguineous relationship between the parents. The inspection of ROH showed that the *GINS2* candidate variant was located in the patient's largest ROH (2.04 Mb) detected through exome sequencing data; only four other smaller ROHs (varying between 1.17 and 1.66 Mb) were detected. Populational data (gnomAD[9]) demonstrated that this variant has an extremely low frequency (0.020%; 7/34 498 in the 'Latino' population), which can be extrapolated using the Hardy-Weinberg equilibrium to a frequency of homozygotes of about $1/9.72\times10^{7}$. Interestingly, the presence of homozygous variants in *GINS2* is extremely rare in gnomAD[9]: so far, only two missense (and no loss-of-function) homozygous variants have been listed. Of note, this is a small gene with an open reading frame of 555 bp.

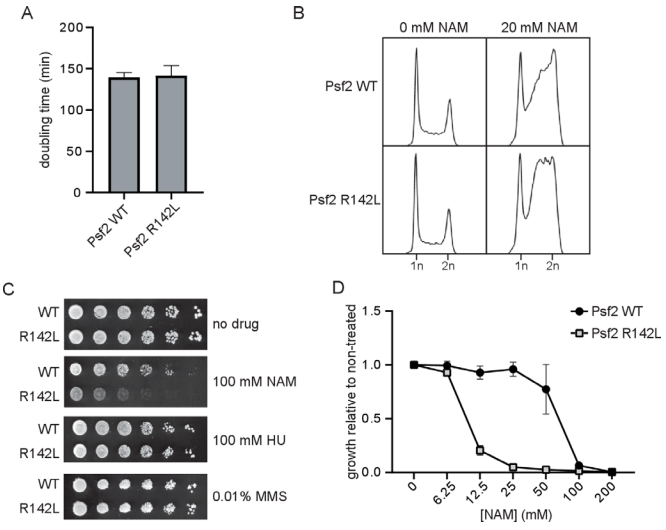

Figure 2 Strains of yeast expressing Psf2-R142L show reduced growth and altered cell cycle progression in the presence of nicotinamide (NAM). (A) OD_{630} of yeast cultures was monitored for 48 hours and doubling time was derived from exponential regression of the resulting growth curve (n=3). (B) Cell cycle profiles of actively replicating yeast cultures were assessed by flow cytometry after 8 hours of growth in the presence or absence of 20 mM NAM. (C) Serial fivefold dilutions of yeast were grown on solid media in the presence or absence of 100 mM NAM, 100 mM hydroxyurea (HU) or 0.01% methyl methanesulfonate (MMS) at 30°C for 72 hours (n=3). (D) Yeasts were cultured for 48 hours in the presence of a range of concentrations of NAM. Growth in the presence of NAM is presented as a fraction of growth in the absence of NAM (n=3). WT, wild type.

Finally, the substitution of the highly conserved arginine (down to yeast, considering 11 species; online supplemental figure 1) by a leucine, corresponding to a moderate physicochemical difference (Grantham dist: 102 (0–215)), is classified by bioinformatic analysis as likely pathogenic (PolyPhen-2, SIFT, MutationTaster). The Combined Annotation Dependent Depletion (CADD) score was 28.3.[10]

Protein structural analysis shows that this missense variant affects one residue (p.Arg114) located in an alpha helix domain and in close proximity to CDC45, MCM5 and GINS3 polypeptides (online supplemental figure 2A). Given the availability of its three-dimensional structure, both from humans and *S. cerevisiae*, we analysed the variant's impact on protein interaction and stability. In different protein structures (or conformations) from *S. cerevisiae*, the corresponding residue—p.Arg142—establishes several hydrogen bonds with other neighbouring amino acids from Psf2 (GINS2) itself but also with Cdc45 (one conserved residue in both species) and Mcm5 (an isofunctionally substituted residue) (online supplemental figure 2B–D). Structure prediction by comparative modelling of protein three-dimensional structures suggested that the arginine to leucine substitution disrupts all of these interactions (online supplemental figure 2E–G).

To evaluate the functional impact of the GINS2 p.(Arg114Leu) substitution, *S. cerevisiae* strains expressing Psf2 p.(Arg142Leu) (Psf2-R142L) were generated. No obvious differences in cell doubling time or cell cycle distribution were observed between strains expressing wild-type Psf2 (Psf2-WT) and those expressing Psf2-R142L on unperturbed growth (figure 2A,B). However, testing the effects of a series of compounds that induce DNA replication stress revealed that nicotinamide (NAM), a compound that causes DNA damage through inhibition of histone deacetylases of the sirtuin family, impaired the growth of Psf2-R142L-expressing cells (figure 2C,D). NAM-induced inhibition of the sirtuins Hst3 and Hst4 causes DNA damage in yeast. Moreover, *hst3*Δ *hst4*Δ double mutation causes synthetic lethality when combined with epitope-tagged versions of DNA replication factors, indicating that subtle defects in DNA replication protein function can be detected using elevated NAM sensitivity as a read-out. While exposure to NAM resulted in the accumulation of cells in late S and G2 phases of the cell cycle for both Psf2-WT and Psf2-R142L-expressing cells (figure 2B), Psf2-R142L-expressing cells accumulated earlier in S phase than those expressing Psf2-WT, indicative of impaired DNA replication. Together, these observations indicate that the GINS2 p.(Arg113Leu) substitution negatively impacts the function of the corresponding protein.

So far, no other patient with *GINS2*-related MGORS has been identified, specifically using GeneMatcher or by contacting experts in this syndrome (see the Acknowledgements section for further details), corroborating the rarity of MGORS caused by pathogenic *GINS2* variants.

DISCUSSION

We describe a patient with growth delay, craniofacial dysmorphisms and craniosynostosis, and in whom a homozygous missense variant in the *GINS2* gene was identified. Although it is classified as of unknown clinical significance using the guidelines proposed by the American College of Medical Genetics and Genomics (ACMG), several lines of evidence support that this variant in *GINS2* is an additional cause of MGORS.

First, the homozygous p.(Arg114Leu) variant in *GINS2* is likely deleterious. This variant was identified in both healthy parents in heterozygosity. Since they are not consanguineous, they may share a very distant common ancestor, which is consistent with the homozygosity data. The high degree of intolerance of *GINS2* to homozygous variants (even of missense type) is suggestive of high selective pressure, thus supporting the possibility of *GINS2* being a disease-causing gene. Additionally, the *in silico* analysis also supported the pathogenicity of the p.(Arg114Leu) substitution, which occurred in a highly conserved residue in GINS2. Finally, modelling of the p.(Arg114Leu) substitution in the budding yeast *S. cerevisiae* showed that in yeast this substitution does not affect growth either under normal conditions or in the presence of hydroxyurea or methyl methanesulfonate, but confers sensitivity to DNA replication stress caused by the histone deacetylase inhibitor NAM, consistent with partially defective functions of Psf2 (yeast GINS2).

Second, this novel *GINS2* variant was identified in an individual with clinical features reminiscent of MGORS (online supplemental tables 3 and 4). She has the cardinal features of this syndrome, such as prenatal and postnatal growth restriction, patellar hypoplasia, microtia and coronal craniosynostosis. Additionally, she has overlapping skeletal, cardiac, gastrointestinal and anal abnormalities, and normal intelligence.

Third, the functional interactions of GINS2 and its role in DNA replication strengthen its causality in MGORS. GINS2 (OMIM*610609; GINS complex subunit 2) is part of the tetrameric GINS complex—composed of GINS1/GINS2/GINS3/GINS4—which is conserved in eukaryotes, from *S. cerevisiae* to *Homo sapiens*.[11–13] This complex was shown to play an essential role in the initiation of DNA replication and progression of DNA replication forks,[11 12] unwinding DNA for polymerase epsilon and binding preferentially to single-stranded DNA in the replicative helicase complex.[14] The GINS tetramer interacts

with CDC45 and MCM proteins to form the CMG helicase. The p.(Arg114Leu) substitution is located at the docking site of MCM5 and CDC45 at GINS2, which involves its N-terminal B-domain and its helical domain.[15] The analysis of protein structural data suggested that this novel variant might compromise the interaction between GINS2 and both CDC45 and MCM5. Considering these subtle changes, we anticipated that the p.(Arg114Leu) missense variant might be hypomorphic, thus maintaining the partial function of GINS2. This is supported by the analysis of the equivalent Psf2-R142L substitution in yeast, which exhibited normal growth in several experimental conditions but a specific defect when exposed to NAM (figure 2).

Indeed, deletion of Psf1 in mice (*GINS1* in humans) results in early embryonic lethality.[12] Of note, Psf1 is largely expressed in active stem cell systems in mice, including adult bone marrow, thymus, testis and ovary, but not the remaining adult tissues.[12] Interestingly, five patients with compound heterozygous variants in *GINS1* were reported with neutropenia, natural killer cell deficiency and growth delay.[16] Missense variants and variants located in the *5′* untranslated region resulted in lower GINS1 levels in patients' cells, which showed impaired GINS complex assembly, basal replication stress, impaired checkpoint signalling, defective cell cycle control and genomic instability, which could be rescued by wild-type GINS1.[16] Although our patient did not present immunodeficiency, growth retardation was evident, in particular in utero and during early infancy.

Our patient's phenotype is strikingly similar to the phenotype of individuals with *CDC45* variants, particularly those who presented with craniosynostosis and mild MGORS features. Interestingly, pathogenic homozygous or compound heterozygous variants in the *CDC45* gene result in the distinctive MGORS clinical triad and frequently in craniosynostosis (OMIM#617063; MGORS7).[5] Noteworthy, our patient had both patellae, though hypoplastic, and short stature was mild. Additionally, she developed cardiac and anal abnormalities. Also, pathogenic variants in *MCM5* and *MCM4*, other genes of the CMG helicase complex, were respectively associated with MGORS[6] and a distinct growth delay phenotype.[17–20] Based on the functional interaction between the CMG complex and DNA polymerases, we propose that changes in this complex would affect DNA replication as a possible pathophysiological mechanism for *GINS2*-related MGORS. In line with this assumption, biallelic hypomorphic missense variants in *GINS3* have been reported just recently, as an additional molecular cause of MGORS, suggesting defects in *GINS* genes as a cause of this clinical entity (Kannu *et al*, personal communication, 2020).

In summary, we report an individual with a homozygous likely disease-causing variant in *GINS2* and with clinical features overlapping those of MGORS, including prenatal and postnatal growth delay, hypoplastic patellae and typical craniofacial dysmorphisms, such as microtia and craniosynostosis. The recognition of the *GINS2* gene as a novel causative gene of MGORS is crucial for the anticipatory multidisciplinary care of affected individuals, as well as for genetic counselling, enabling parents the possibility of prenatal or preimplantation diagnosis. The apparent rarity of *GINS2* variants associated with MGORS may be explained because the phenotype arises only in a narrow window of disturbed GINS2 function, intermediate between lethal and normal outcomes.

Author affiliations
[1]Department of Human Genetics, Radboud University Medical Center and Donders Institute for Brain, Cognition and Behaviour, Nijmegen, The Netherlands
[2]Unit for Multidisciplinary Research in Biomedicine, Instituto de Ciências Biomédicas Abel Salazar, Universidade do Porto, Porto, Portugal
[3]Clinical Genetics Group, MRC Weatherall Institute of Molecular Medicine, University of Oxford, Oxford, UK
[4]Maisonneuve-Rosemont Hospital Research Center, Montréal, Québec, Canada
[5]Centre for Predictive and Preventive Genetics (CGPP), Institute for Molecular and Cell Biology (IBMC), Universidade do Porto, Porto, Portugal
[6]UnIGENe, i3S - Instituto de Investigação e Inovação em Saúde, Universidade do Porto, Porto, Portugal

Acknowledgements The authors are very thankful to the proband and her family for their collaboration, which was fundamental for publishing this work. The authors would like to acknowledge the collaboration of Sonja de Munnik (Radboudumc, Nijmegen, The Netherlands), Ernie Bongers (Radboudumc, Nijmegen, The Netherlands) and Louise Bicknell (University of Otago, Dunedin, New Zealand), who informed the authors of the absence of individuals with biallelic *GINS2* variants in their Meier-Gorlin cohorts.

Contributors MJNS collected the patient data and summarised the clinical and genetic findings. KAM, NK and AOMW performed and analysed the exome sequencing. JO participated in the bioinformatic data interpretation. HW and MM designed, performed and interpreted all functional assays. MJNS drafted the manuscript and APMdB, AOMW, MM, HW and JO participated in final draft revisions. All coauthors critically reviewed the manuscript and approved the final submitted version.

Funding Core facilities were supported by the WIMM Strategic Alliance (G0902418 and MC_UU_12025). This work was supported by the National Institute for Health Research (NIHR) Oxford Biomedical Research Centre Programme (AOMW), a Wellcome Senior Investigator Award 102731 (AOMW) and the Canadian Institute for Health Research PJT 159683 (HW).

Competing interests None declared.

Patient consent for publication Parental/guardian consent obtained.

Ethics approval The Genetics Basis of Craniofacial Malformations study was approved by the London-Riverside Research Ethics Committee, UK (reference 09/H0706/20). The study was conducted in accordance with the Declaration of Helsinki Ethical Principles.

Provenance and peer review Not commissioned; externally peer reviewed.

ORCID iDs
Maria J Nabais Sá http://orcid.org/0000-0002-9472-6050
Andrew O M Wilkie http://orcid.org/0000-0002-2972-5481
Jorge Oliveira http://orcid.org/0000-0003-3924-6385

REFERENCES

1 de Munnik SA, Bicknell LS, Aftimos S, Al-Aama JY, van Bever Y, Bober MB, Clayton-Smith J, Edrees AY, Feingold M, Fryer A, van Hagen JM, Hennekam RC, Jansweijer MCE, Johnson D, Kant SG, Opitz JM, Ramadevi AR, Reardon W, Ross A, Sarda P, Schrander-Stumpel CTRM, Schoots J, Temple IK, Terhal PA, Toutain A, Wise CA, Wright M, Skidmore DL, Samuels ME, Hoefsloot LH, Knoers NVAM, Brunner HG, Jackson AP, Bongers EMHF. Meier-Gorlin syndrome genotype-phenotype studies: 35 individuals with pre-replication complex gene mutations and 10 without molecular diagnosis. *Eur J Hum Genet* 2012;20:598–606.
2 Bicknell LS, Walker S, Klingseisen A, Stiff T, Leitch A, Kerzendorfer C, Martin C-A, Yeyati P, Al Sanna N, Bober M, Johnson D, Wise C, Jackson AP, O'Driscoll M, Jeggo PA. Mutations in *ORC1*, encoding the largest subunit of the origin recognition complex, cause microcephalic primordial dwarfism resembling Meier-Gorlin syndrome. *Nat Genet* 2011;43:350–5.
3 Bicknell LS, Bongers EMHF, Leitch A, Brown S, Schoots J, Harley ME, Aftimos S, Al-Aama JY, Bober M, Brown PAJ, van Bokhoven H, Dean J, Edrees AY, Feingold M,

Fryer A, Hoefsloot LH, Kau N, Knoers NVAM, Mackenzie J, Opitz JM, Sarda P, Ross A, Temple IK, Toutain A, Wise CA, Wright M, Jackson AP. Mutations in the pre-replication complex cause Meier-Gorlin syndrome. *Nat Genet* 2011;43:356–9.
4 Guernsey DL, Matsuoka M, Jiang H, Evans S, Macgillivray C, Nightingale M, Perry S, Ferguson M, LeBlanc M, Paquette J, Patry L, Rideout AL, Thomas A, Orr A, McMaster CR, Michaud JL, Deal C, Langlois S, Superneau DW, Parkash S, Ludman M, Skidmore DL, Samuels ME. Mutations in origin recognition complex gene Orc4 cause Meier-Gorlin syndrome. *Nat Genet* 2011;43:360–4.
5 Fenwick AL, Kliszczak M, Cooper F, Murray J, Sanchez-Pulido L, Twigg SRF, Goriely A, McGowan SJ, Miller KA, Taylor IB, Logan C, Bozdogan S, Danda S, Dixon J, Elsayed SM, Elsobky E, Gardham A, Hoffer MJV, Koopmans M, McDonald-McGinn DM, Santen GWE, Savarirayan R, de Silva D, Vanakker O, Wall SA, Wilson LC, Yuregir OO, Zackai EH, Ponting CP, Jackson AP, Wilkie AOM, Niedzwiedz W, Bicknell LS, WGS500 Consortium. Mutations in *CDC45*, Encoding an Essential Component of the Pre-initiation Complex, Cause Meier-Gorlin Syndrome and Craniosynostosis. *Am J Hum Genet* 2016;99:125–38.
6 Vetro A, Savasta S, Russo Raucci A, Cerqua C, Sartori G, Limongelli I, Forlino A, Maruelli S, Perucca P, Vergani D, Mazzini G, Mattevi A, Stivala LA, Salviati L, Zuffardi O. *MCM5*: a new actor in the link between DNA replication and Meier-Gorlin syndrome. *Eur J Hum Genet* 2017;25:646–50.
7 Knapp KM, Sullivan R, Murray J, Gimenez G, Arn P, D'Souza P, Gezdirici A, Wilson WG, Jackson AP, Ferreira C, Bicknell LS. Linked-read genome sequencing identifies biallelic pathogenic variants in *DONSON* as a novel cause of Meier-Gorlin syndrome. *J Med Genet* 2020;57:195–202.
8 Fragkos M, Ganier O, Coulombe P, Méchali M. DNA replication origin activation in space and time. *Nat Rev Mol Cell Biol* 2015;16:360–74.
9 Karczewski KJ, Francioli LC, Tiao G, Cummings BB, Alfoldi J, Wang Q, Collins RL, Laricchia KM, Ganna A, Birnbaum DP, Gauthier LD, Brand H, Solomonson M, Watts NA, Rhodes D, Singer-Berk M, England EM, Seaby EG, Kosmicki JA, Walters RK, Tashman K, Farjoun Y, Banks E, Poterba T, Wang A, Seed C, Whiffin N, Chong JX, Samocha KE, Pierce-Hoffman E, Zappala Z, O'Donnell-Luria AH, Minikel EV, Weisburd B, Lek M, Ware JS, Vittal C, Armean IM, Bergelson L, Cibulskis K, Connolly KM, Covarrubias M, Donnelly S, Ferriera S, Gabriel S, Gentry J, Gupta N, Jeandet T, Kaplan D, Llanwarne C, Munshi R, Novod S, Petrillo N, Roazen D, Ruano-Rubio V, Saltzman A, Schleicher M, Soto J, Tibbetts K, Tolonen C, Wade G, Talkowski ME, Genome Aggregation Database Consortium. Neale BM, Daly MJ, MacArthur dG. The mutational constraint spectrum quantified from variation in 141,456 humans. *Nature* 2020;581:434–43.
10 Rentzsch P, Witten D, Cooper GM, Shendure J, Kircher M. CADD: predicting the deleteriousness of variants throughout the human genome. *Nucleic Acids Res* 2019;47:D886–94.
11 Takayama Y, Kamimura Y, Okawa M, Muramatsu S, Sugino A, Araki H. Gins, a novel multiprotein complex required for chromosomal DNA replication in budding yeast. *Genes Dev* 2003;17:1153–65.
12 Ueno M, Itoh M, Kong L, Sugihara K, Asano M, Takakura N. Psf1 is essential for early embryogenesis in mice. *Mol Cell Biol* 2005;25:10528–32.
13 Aparicio T, Guillou E, Coloma J, Montoya G, Méndez J. The human GINS complex associates with Cdc45 and MCM and is essential for DNA replication. *Nucleic Acids Res* 2009;37:2087–95.
14 Li H, O'Donnell ME. The eukaryotic CMG helicase at the replication fork: emerging architecture reveals an unexpected mechanism. *Bioessays* 2018;40.
15 Simon AC, Sannino V, Costanzo V, Pellegrini L. Structure of human Cdc45 and implications for CMG helicase function. *Nat Commun* 2016;7:11638.
16 Cottineau J, Kottemann MC, Lach FP, Kang Y-H, Vély F, Deenick EK, Lazarov T, Gineau L, Wang Y, Farina A, Chansel M, Lorenzo L, Piperoglou C, Ma CS, Nitschke P, Belkadi A, Itan Y, Boisson B, Jabot-Hanin F, Picard C, Bustamante J, Eidenschenk C, Boucherit S, Aladjidi N, Lacombe D, Barat P, Qasim W, Hurst JA, Pollard AJ, Uhlig HH, Fieschi C, Michon J, Bermudez VP, Abel L, de Villartay J-P, Geissmann F, Tangye SG, Hurwitz J, Vivier E, Casanova J-L, Smogorzewska A, Jouanguy E. Inherited GINS1 deficiency underlies growth retardation along with neutropenia and NK cell deficiency. *J Clin Invest* 2017;127:1991–2006.
17 Eidenschenk C, Dunne J, Jouanguy E, Fourlinnie C, Gineau L, Bacq D, McMahon C, Smith O, Casanova J-L, Abel L, Feighery C. A novel primary immunodeficiency with specific natural-killer cell deficiency maps to the centromeric region of chromosome 8. *Am J Hum Genet* 2006;78:721–7.
18 Gineau L, Cognet C, Kara N, Lach FP, Dunne J, Veturi U, Picard C, Trouillet C, Eidenschenk C, Aoufouchi S, Alcaïs A, Smith O, Geissmann F, Feighery C, Abel L, Smogorzewska A, Stillman B, Vivier E, Casanova J-L, Jouanguy E. Partial *MCM4* deficiency in patients with growth retardation, adrenal insufficiency, and natural killer cell deficiency. *J Clin Invest* 2012;122:821–32.
19 Hughes CR, Guasti L, Meimaridou E, Chuang C-H, Schimenti JC, King PJ, Costigan C, Clark AJL, Metherell LA. *MCM4* mutation causes adrenal failure, short stature, and natural killer cell deficiency in humans. *J Clin Invest* 2012;122:814–20.
20 Casey JP, Nobbs M, McGettigan P, Lynch S, Ennis S. Recessive mutations in *MCM4/PRKDC* cause a novel syndrome involving a primary immunodeficiency and a disorder of DNA repair. *J Med Genet* 2012;49:242–5.

SUPPLEMENTARY METHODS

Exome sequencing analysis

Using DNA extracted from peripheral blood cells of the proband and both parents, exome capture of DNA was carried out using the SureSelect Human All Exon Kit v6 (Agilent) following the manufacturer's instructions. We generated a library for each sample using 3 µg DNA extracted from whole blood. Exome sequencing was performed on an Illumina HiSeq 4000, with 150 bp paired-end reads. The reads were mapped to the GRCh38 reference genome and artefacts excluded, as previously described.[1] We analysed the data assuming complete penetrance, allowing for the possibility of either a *de novo* mutation (dominant) or biallelic inheritance (recessive). We used a custom Platypus 0.8.1[2] Bayesian script to identify *de novo* mutations, and a script using bcftools 1.5 with the 1000G genetic map for calling regions of homozygosity. To identify biallelic variants we filtered on a minor allele frequency of <0.001 (The Genome Aggregation Database, gnomAD).[3] All variants called were checked by examining individual reads in GBrowse[4] and nonsynonymous variants assigned priority based on estimates of deleteriousness using Deleterious scores[5] and CADD scores.[6] Literature review of biochemistry data and the protein's functional association network was carried out to support a possible pathophysiological mechanism of a novel gene linked to MGORS.

Prediction of mutation impact on protein structure

To conduct *in silico* protein analysis the human (protein data bank, PDB ID: 6XTX[7]) and Saccharomyces cerevisiae (PDB IDs: 6SKL[8] and 3JC5[9]) CMG structures were retreived and visualized using both: i) Mol* (doi:10.2312/molva.20181103) tool imbedded in RCSB PDB, and ii) Maestro software (version 12.2.012, MMshare Version 4.8.012, Release 2019-4, Platform Darwin-x86_64). Structural prediction of wild-type GINS2/PSF2 and mutated

sequences was done using Maestro, HHPRED and MODeller softwares[10] for protein homology detection and structure prediction by comparative modeling of protein three-dimensional structures.

Yeast strains and growth conditions

Yeast strains used in this study are listed in Supplementary Table 5. Yeast strains were constructed and propagated using standard genetic methods. Yeast were cultured in YPD supplemented with adenine and incubated at 30˚C, unless otherwise indicated.

Generation of yeast strains

The *PSF2* gene, along with 500 bp of upstream and downstream sequence, was amplified from the genome of yeast BY4743 using primers p416-PSF2_Fwd and p416-PSF2_Rev and cloned into the plasmid p416GDP by gap repair to generate the plasmid p416-PSF2-WT (for primer sequences, see Supplementary Table 6). Site-directed mutagenesis of p416-PSF2-WT was performed using primers PSF2-R142L_Fwd and PSF2-R142L_Rev to generate plasmid p416-psf2-R142L. To generate cassettes of the 3' end of the *PSF2* gene linked to the *kanMX6* cassette for transformation of yeast, the 3' ends of *PSF2* from p416-PSF2-WT and p416-psf2-R142L were amplified using primers PSF2-C and PSF2-D, and the *kanMX6* cassette was amplified from pFA6a-kanMX6 [11] using primers PSF2-F2-STOP and PSF2-R1.[12] The PCR products of both reactions were then pooled and amplified with primers PSF2-C and PSF2-R1 to generate the cassettes 3'-*PSF2-WT::kanMX6* and *3'-psf2-R142L::kanMX6*, both of which encode the 3' end of the *PSF2* gene linked to the *kanMX6* cassette. Cassettes were used to transform yeast strain BY4741 to G418 resistance, and *PSF2* genes of isolates were sequenced by Sanger sequencing to confirm absence of undesired mutations.

Measurement of DNA content by flow cytometry

Cells were cultured for 8 hours at a density of less than 0.2 OD_{630} in the presence or absence of 20 mM NAM. Cells were fixed in 70% ethanol. Prior to analysis by flow cytometry, fixed cells were sonicated for 10 seconds at 30% duty cycle (Branson Digital Sonifier 450) and treated with 0.4 µg/mL RNAse A in 50 mM Tris-HCl pH 7.5 at 42˚C for 3 hours, followed by 1 mg/mL Proteinase K in 50 mM Tris-HCl pH 7.5 at 50˚C for 30 minutes. Cells were stained with Sytox Green (Invitrogen) to assess DNA content as previously described.[13] Analysis was performed using a FACS Calibur flow cytometer with CellQuest Pro software (BD Biosciences). Further analyses were performed using FlowJo software (version 10.6.2, BD Biosciences).

Assay for cell doubling time

Yeast cultures were diluted to OD_{630} 0.001 and 100 µL aliquots were transferred to a 96-well plate. Cultures were incubated at 30˚C for 48 hours in a BioTek ELx800 plate reader with Gen5 software (ver 2.09, BioTek Instruments). Culture density was monitored at 30 minute intervals by measuring the OD_{630} after 30 seconds of agitation to ensure that cells were homogenously mixed. Doubling times were derived from exponential regression of the resulting growth curve.

Drug susceptibility assay

Yeast cultures were diluted to the same OD_{630}, and 100 µL aliquots placed in a 96-well plate. A series of 5-fold dilutions was prepared, and spotted onto the indicated solid media using a replica plater tool (Sigma-Aldrich). Growth of yeast was recorded every 24 hours for 4 days.

Assay for minimum inhibitory concentration of NAM

Yeast cultures were diluted to 0.0005 OD_{630} and 100 µL aliquots were incubated in 96-well with a range of concentrations of nicotinamide (NAM). NAM is a compound that causes DNA damage through inhibition of histone deacetylases of the sirtuin family.[14] NAM-induced inhibition of the sirtuins Hst3 and Hst4 causes DNA damage in yeast.[14,15] Moreover, *hst3*Δ *hst4*Δ double mutation causes synthetic lethality when combined with epitope-tagged versions of DNA replication factors,[16,17] indicating that subtle defects in DNA replication protein function can be detected using elevated NAM sensitivity as a readout. OD_{630} was measured after 48 hours using an EL800 plate reader with Gen5 software (ver 2.09, BioTek Instruments). Growth of yeast was normalized to an untreated control well for each strain.

References:

1. Miller KA, Twigg SR, McGowan SJ, Phipps JM, Fenwick AL, Johnson D, Wall SA, P Noons, Rees KEM, Tidey EA, Craft J, Taylor J, Taylor JC, Goos JAC, Swagemakers SMA, Mathijssen IMJ, van der Spek PJ, Lord H, Lester T, Abid N, Cilliers D, Hurst JA, Morton JEV, Sweeney E, Weber A, Wilson LC, Wilkie AOM. Diagnostic value of exome and whole genome sequencing in craniosynostosis. *J Med Genet* 2017;54:260-68.

2. Rimmer A, Phan H, Mathieson I, Iqbal Z, Twigg SRF; WGS500 Consortium, Wilkie AOM, McVean G, Lunter G. Integrating mapping-, assembly- and haplotype-based approaches for calling variants in clinical sequencing applications. *Nat Genet* 2014;46:912-918.

3. Karczewski KJ, Francioli LC, Tiao G, Cummings BB, Alfoldi J, Wang Q, Collins RL, Laricchia KM, Ganna A, Birnbaum DP, Gauthier LD, Brand H, Solomonson M, Watts NA, Rhodes D, Singer-Berk M, England EM, Seaby EG, Kosmicki JA, Walters RK, Tashman K, Farjoun Y, Banks E, Poterba T, Wang A, Seed C, Whiffin N, Chong JX, Samocha KE, Pierce-Hoffman E, Zappala Z, O'Donnell-Luria AH, Minikel EV, Weisburd B, Lek M, Ware JS, Vittal C, Armean IM, Bergelson L, Cibulskis K, Connolly KM, Covarrubias M, Donnelly S, Ferriera S, Gabriel S, Gentry J, Gupta N, Jeandet T, Kaplan D, Llanwarne C, Munshi R, Novod S, Petrillo N, Roazen D, Ruano-Rubio V, Saltzman A, Schleicher M, Soto J, Tibbetts K, Tolonen C, Wade G, Talkowski ME, Genome Aggregation Database Consortium; Neale BM, Daly MJ, MacArthur DG. The mutational constraint spectrum quantified from variation in 141,456 humans. *Nature* 2020;581:434-443.

4. Stein LD, Mungall C, Shu S, Caudy M, Mangone M, Day A, Nickerson E, Stajich JE, Harris TW, Arva A, Lewis S. The generic genome browser: a building block for a model organism system database. *Genome Res* 2002;12:1599-610.

5. Calpena E, Cuellar A, Bala K, Swagemakers SMA, Koelling N, McGowan SJ, Phipps JM, Balasubramanian M, Cunningham ML, Douzgou S, Lattanzi W, Morton JEV, Shears D, Weber A, Wilson LC, Lord H, Lester T, Johnson D, Wall SA, Twigg SRF, Mathijssen IMJ, Boardman-Pretty F; Genomics England Research Consortium, Boyadjiev SA, Wilkie AOM. *SMAD6* variants in craniosynostosis: genotype and phenotype evaluation. *Genet Med* 2020;22:1498-506.

6. Rentzsch P, Witten D, Cooper GM, Shendure J, Kircher M. CADD: predicting the deleteriousness of variants throughout the human genome. *Nucleic Acids Res* 2019;47:D886-D894.

7. Rzechorzek NJ, Hardwick SW, Jatikusumo VA, Chirgadze DY, Pellegrini L. CryoEM structures of human CMG-ATPgammaS-DNA and CMG-AND-1 complexes. *Nucleic Acids Res* 2020;48:6980-6995.

8. Baretic D, Jenkyn-Bedford M, Aria V, Cannone G, Skehel M, Yeeles JTP. Cryo-EM Structure of the Fork Protection Complex Bound to CMG at a Replication Fork. *Mol Cell* 2020;78:926-940.e13.

9. Yuan Z, Bai L, Sun J, Georgescu R, Liu J, O'Donnell ME, Li H. Structure of the eukaryotic replicative CMG helicase suggests a pumpjack motion for translocation. *Nat Struct Mol Biol* 2016;23:217-24.

10. Zimmermann L, Stephens A, Nam SZ, Rau D, Kubler J, Lozajic M, Gabler F, Soding J, Lupas AN, Alva V. A Completely Reimplemented MPI Bioinformatics Toolkit with a New HHpred Server at its Core. *J Mol Biol* 2018;430:2237-2243.

11. Bähler J, Wu J-Q, Longtine MS, Shah NG, McKenzie A, Steever AB, Wach A, Philippsen P, Pringle JR. Heterologous modules for efficient and versatile PCR-based gene targeting in *Schizosaccharomyces pombe*. *Yeast* 1998;14:943-951.

12. Longtine MS, McKenzie A, Demarini DJ, Shah NG, Wach A, Brachat A, Philippsen P, Pringle JR. Additional modules for versatile and economical PCR-based gene deletion and modification in *Saccharomyces cerevisiae*. *Yeast* 1998;14:953-961.

13. Haase SB, Reed SI. Improved flow cytometric analysis of the budding yeast cell cycle. *Cell Cycle* 2002;1:117-121.

14. Simoneau A, Ricard É, Weber S, Hammond-Martel I, Wong LH, Sellam A, Giaever G, Nislow C, Raymond M, Wurtele H. Chromosome-wide histone deacetylation by sirtuins prevents hyperactivation of DNA damage-induced signaling upon replicative stress. *Nucleic Acids Res.* 2016;44:2706-26.

15. Celic I, Masumoto H, Griffith WP, Meluh P, Cotter RJ, Boeke JD, Verreault A. The sirtuins hst3 and Hst4p preserve genome integrity by controlling histone h3 lysine 56 deacetylation. *Curr Biol.* 2006;16:1280-9.

16. Celic I, Verreault A, Boeke JD. Histone H3 K56 hyperacetylation perturbs replisomes and causes DNA damage. *Genetics.* 2008;179:1769-84.

17. Simoneau A, Delgoshaie N, Celic I, Dai J, Abshiru N, Costantino S, Thibault P, Boeke JD, Verreault A, Wurtele H. Interplay between histone H3 lysine 56 deacetylation and chromatin modifiers in response to DNA damage. *Genetics.* 2015;200:185-205.

Supplementary table 1. Length/height, weight and head circumference of girl with a homozygous missense *GINS2* variant.

Age	Lenght/height (cm)	Pct	SD	Weight (kg)	Pct	SD	Head circumference (cm)	Pct	SD
Birth	47	14	-1.10	2.260	1	-2.22	30.5	< 1	-2.92
3 months	57	18	-0.90	4.270	3	-1.85	36	< 1	-3.08
6 months	62	12	-1.19	5.210	1	-2.51	39	< 1	-2.76
9 months	65	5	-1.69	5.760	< 1	-3.15	42	6	-1.55
12 months	68	3	-1.89	6.640	< 1	-3.10	43	6	-1.60
18 months	73.5	2	-2.02	7.510	< 1	-3.42	45.3	19	-0.88
22 months	79	8	-1.39	8.400	< 1	-3.08	45.5	12	-1.19
2y 9m	87.2	7	-1.45	10,500	1	-2.24	46.5	12	-1.19
3y 2m	89.5	7	-1.50	11.400	3	-1.96	47.6	24	-0.72
3y 6m	92.5	11	-1.21	11.000	1	-2.53	NA	na	na
4y 1m	96.7	16	-1.00	12.400	2	-2.10	NA	na	na
5y	101.7	11	-1.20	12.950	1	-2.51	NA	na	na
5y 7m	105.7	12	-1.16	14.200	1	-2.31	NA	na	na
6y	111	26	-0.64	15.100	1	-2.19	NA	na	na
7y	117.5	26	-0.64	17.300	3	-1.95	NA	na	na

Pct, Percentile. SD, Standard deviation. y, years. m, months. NA, not available. na, not applicable.
Reference: https://simulconsult.com/resources/measurement.html

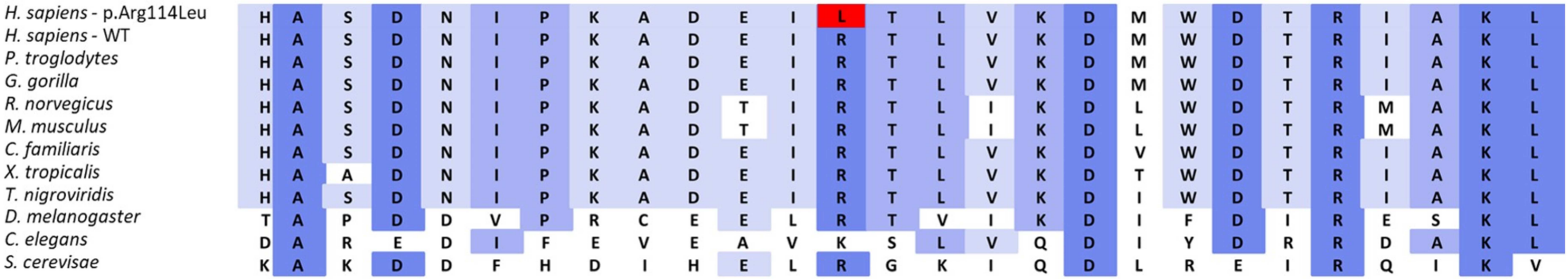
H. sapiens - p.Arg114Leu H A S D N I P K A D E I L T L V K D M W D T R I A K L
H. sapiens - WT H A S D N I P K A D E I R T L V K D M W D T R I A K L
P. troglodytes H A S D N I P K A D E I R T L V K D M W D T R I A K L
G. gorilla H A S D N I P K A D E I R T L V K D M W D T R I A K L
R. norvegicus H A S D N I P K A D T I R T L I K D L W D T R M A K L
M. musculus H A S D N I P K A D T I R T L I K D L W D T R M A K L
C. familiaris H A S D N I P K A D E I R T L V K D V W D T R I A K L
X. tropicalis H A A D N I P K A D E I R T L V K D T W D T R I A K L
T. nigroviridis H A S D N I P K A D E I R T L V K D I W D T R I A K L
D. melanogaster T A P D D V P R C E E L R T V I K D I F D I R E S K L
C. elegans D A R E D I F E V E A V K S L V Q D I Y D R R D A K L
S. cerevisae K A K D D F H D I H E L R G K I Q D L R E I R Q I K V

Supplementary figure 2A

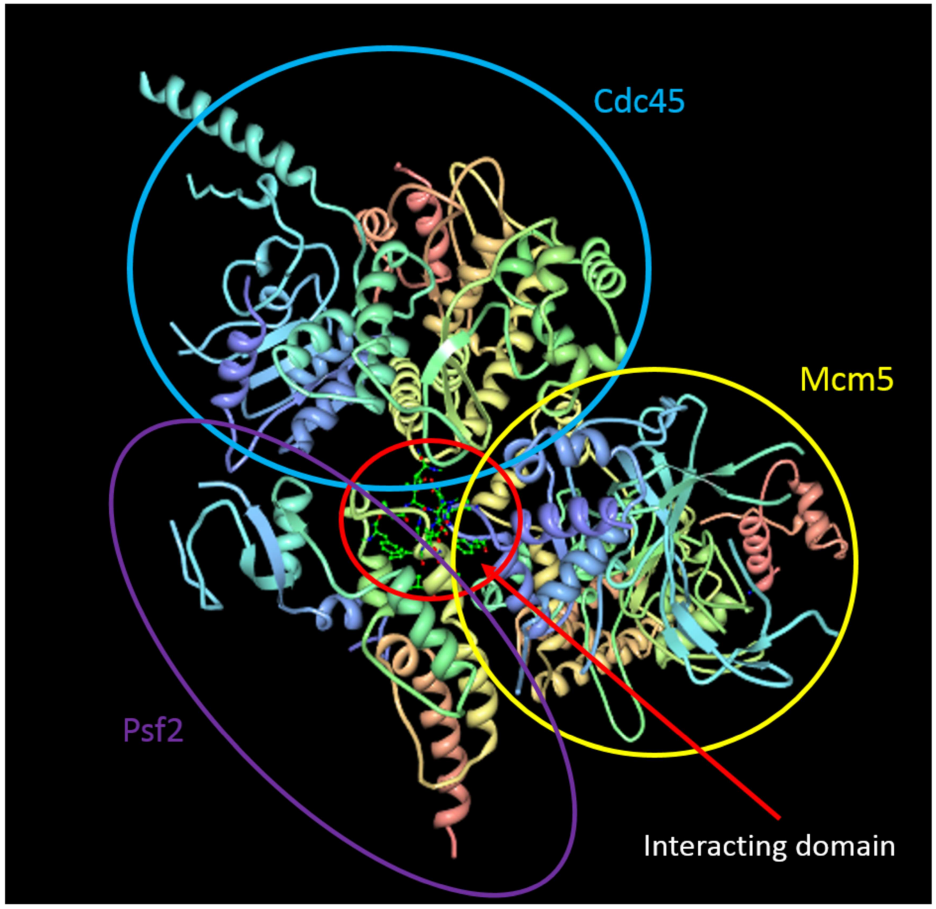

Mcm5 interactions:

NP_006730.2	44	VGTDRTGFTFKYRDELKRHYNLGEYWIEVEMEDLASFDEDLADYLYKQPA	93
XP_001156025.1	44	VGTDRTGFTFKYRDELKRHYNLGEYWIEVEMEDLASFDEDLADYLYKQPA	93
XP_005626282.1	1	------MVMMWAQDELKRHYNLGEYWVEVEMEDLASFDEDLADYLYKQPA	44
NP_001068758.1	44	VGTDRTGFTFKYRDELKRHYNLGEYWIEVEMEDLASFDEELADYLYKQPA	93
NP_032592.2	44	VGTDRTGFTFKYRDELKRHYNLGEYWIEVEMEDLASFDEELADHLHKQPA	93
NP_001099640.1		----------	
NP_001006243.1	44	VGTDRTGFTFKYRDELKRHYNLGQYWVEVEMEDLASFDEDLADYLYKQPT	93
NP_848523.2	45	VGTDRTGFTYKYRDELKRHYTLGEYWIEVEMEDLASFDEDLSDCLYKLPS	94
NP_524308.2	42	---NEENFFYKYRDTLKRNYLNGRYFLEIEMEDLVGFDETLADKLNKQPT	88
XP_313694.2	43	---CEANFSYKYRDTLKRNYLLGRYYLEVEIEDLAGFDESLADKLYKQPT	89
NP_497858.1	47	---STGGFGMIYRDQLKRNYFSHEYRLEINLNHLKNFDEDIEMKLRKFPG	93
NP_013376.1	39	----RLDSQFIYRDQLRNNILVKNYSLTVNMEHLIGYNEDIYKKLSDEPS	84
XP_453475.1	39	----RLDSNFVYREQLRNNLLVHKYFLDVNTEHLIGYNEDLYKKLQDEPI	84
NP_986942.1	39	----RLDARFVYREQLRNNLLVRRYALRVNTEHLIGYNEALYKLVRDEPV	84
XP_001713071.1	42	----VIDNDFIYRTQLRDNLVVKQYMLNIDLRHLISYNEDLAHLLLSQPT	87
XP_003711077.1	38	----RLENKFIYRDQLRENALLGAYYCDVNIGDLIKFNEELAHRIVTEPT	83
XP_961537.1	41	----RLDNSFIYRDQLRENALLKKYYCDVNIGDLIKFNEEIAHRLVTEPA	86
NP_178812.1	43	---EIEQNCFPYREALLDN----PKRLVVHLEDLLSFDSDLPSLIRSAPA	85
NP_001048396.1	47	---TGPTGDFPYRESLVHN----RDHVTVAIEDLDAFDAELSDKIRKSPA	89
NP_001017327.2	45	VGTDRTGFTFKYRDELKRHYNLGEYWIEVEMEDLASFDEDLADYLYKQPT	94

Cdc45 interactions:

NP_001171481.1	297	VDCTRISFEYDLRLVLYQHWSLHDSLCNTSYTAARFKLWSVHGQKRLQEF	346
XP_003317140.1	297	VDCTRISFEYDLRLVLYQHWSLHDSLCNTSYTAARFKLWSVHGQKRLQEF	346
XP_001104872.2	297	VDCTRISFEYDLRLALYQHWSLHDSLCNTSYTAARFKLWSVHGQKRLQEF	346
XP_543547.3	268	VDCTRISFEYDLRLALYQHWSLHDSLCNTCYTAARFKLWSVHGQKRLQEF	317
NP_001019661.1	266	VDCARISFEYDLRLALYQHWSLHDSLCNTCYTAARLQLWSLHGQKRLQEF	315
NP_033992.2	265	VDCTRISFEYDLCLVLYQHWSLHESLYNTSYTAARFKLWSVHGQKRLQEF	314
NP_001099336.1	269	VDCTRISFEYDLCLVLYQHWSLHESLYNTSYTAARFKLWSVHGQKRLQEF	318
XP_415070.2	265	IDCMRIAFEYDLRLALYQHWSLYESLCNTSYTSATLKLWSVQGQKRLQEF	314
NP_998551.1	271	IDCMRINFEYDLRLVLYQHWSLYESICNSCYTSCSFKLWSINGQKKLQEF	320
NP_569880.1	278	MSASKITFENDLHLVLYRHWPVTESMRYSRYSSCQLKLWTLRGEKRLHEL	327
XP_320573.1	278	QTSVKIVFESDLQLALFRHWSVLDSLRYSYYPACRLKLWTHKGDKQMNEL	327
NP_497756.2	267	DDLLHITFGRELPLALYSHWDLFSAMMVSEYFSIKTKNWTQKGDVNIRHL	316
NP_013204.1	313	PDTLTLNIQPDYYLFLLRHSSLYDSFYYSNYVNAKLSLWNENGKKRLHKM	362
XP_455970.1	316	PDSLNLEIRPDYSLFLLRHTSLYDSFYYSNYVNAKLSLWNENGKKRLHKM	365
NP_986736.1	281	ADKLSIDVRPDYLLFLMRHSSLYDSFFYSNYVNARLSLWNENGKKRFHKM	330
NP_594693.1	302	PHDQSIRLEDEFRFMLVRHWSLYDSMLHSAYVGSRLHIWSEEGRKRLHKL	351
XP_003714523.1	449	PEDTSIRLSPEPKFLLIRHWSLYDSMLHSPYLFSRLKMWSETGLKRLHKL	498
XP_957455.1	429	PEDTSIRLSPEPKFLLIRHWSLYDSMLHSPYLFSRLKTWSEAGMKRLHKL	478
NP_189146.1	298	PDCSRISYEEEPRLMLLREWTLFDSMLCSSYIATKLKTWSDNGIKKLKLL	347
NP_001065635.1	302	PEASRIAYEDEPRLMLLREWSLFDSMLCSSYVATKLKTWSDNGLKKLKLL	351
NP_001066041.1	302	PEASRIAYEDEPRLMLLREWSLFDSMLCSSYVATKLKTWSDNGLKKLKLL	351
XP_004910630.1	268	IDCMRIAFEYDLRLSLYQHWSLYESICNSCYTSASLKLWSVQGQKKLQEF	317

Supplementary figure 2B

```
NP_057179.1      ----------MDAAEVEFLAEKELVTIIPNFSLDKIYLIGGD------------------ 32
NP_012463.1      MSLPAHLQQTFSPEEIQFIVENEPIKIFPRITTRQK-IRGDDRGTGNHTRWQLITTDDKA 59
                           :.  *::*:.*:* :.*:*.::  :  : *.*

NP_057179.1      LGPFNPGLPVEVPLWLAINLKQRQKCRLLPPEWMDVEKLEKMRDHER-KEETFTPMPSPY 91
NP_012463.1      LNNMVAMRSTEVVLWIALLLKQQSKCSIVAPQWLTTKELDRKIQYEKTHPDRFSELPWNW 119
                 *. :     .** **:*: ***:.** :: *:*: .::*::  ::*: : : *: :*  :

NP_057179.1      YMELTKLLLNHASDNIPK-ADEIRTLVKDMWDTRIAKLRVSADSFVRQQEAHAKLDNLTL 150
NP_012463.1      -LVLARILFNKAKDDFHDPIHELRGKIQDLREIRQIK---VLKGLKYLNESHLQLDNLSL 175
                  : *:::*:*:*.*:: .  .*:*  ::*: : *  *     ..:   :*:* :****:*

NP_057179.1      MEINTSGTFLTQALNHMYKLRTNLQPLES-TQSQDF--  185
NP_012463.1      LEINELRPFITEIMDKLREIHTASLTAGTENDEEEFNI  213
```

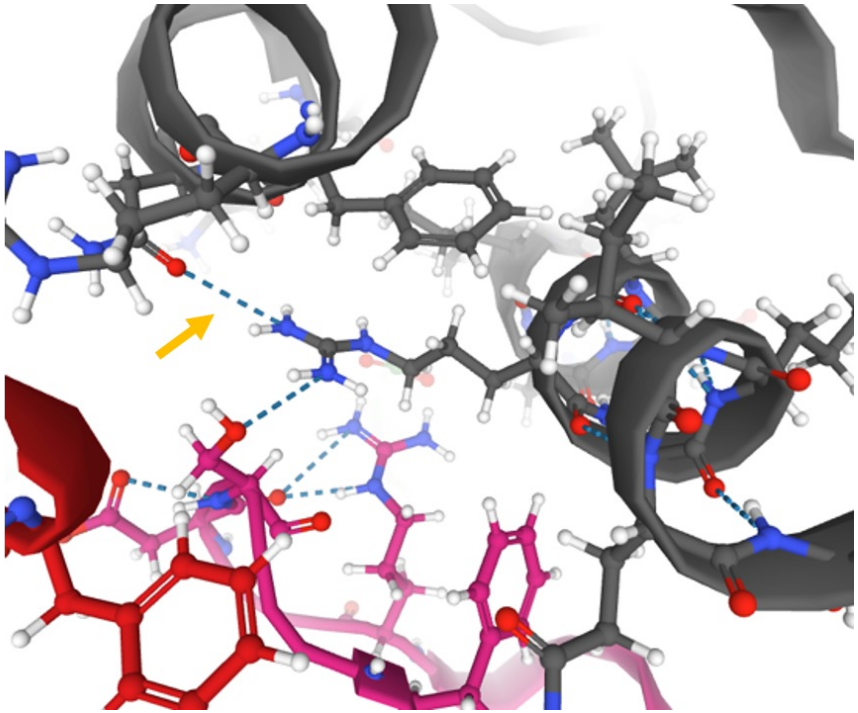

Supplementary figure 2C

```
Query  5    ISQFSEAYNKILRNSSSHSSCQLVIFVSCLNIDALCATKMLSLLFKKQLVQSQIVPIFGY  64
            +S F + + +++++       ++++FV+  ++DALCA K+L  LF+   VQ  +VP+ G+
Sbjct  3    VSDFRKEFYEVVQSQ------RVLLFVAS-DVDALCACKILQALFQCDHVQYTLVPVSGW  55

Query  65   SELRRHYSQLDDNINSLLLVGFGGVIDLEAFLEIDPQEYVIDTDEKSGEQSFRRDIYVLD  124
             EL   + +  +  +L+  G  +DL   L+  P E  I               +V D
Sbjct  56   QELETAFLEHKEQFHYFILINCGANVDLLDILQ--PDEDTI--------------FFVCD  99

Query  125  AHRPWNLDNIFGSQIIQCFDDGTVDDTLGEQKEAYYKLLELDEESGDDELSGDENDNNGG  184
             HRP N+ N++    I+       DD L  +  AY  +   +EE  D+E SG+++D +
Sbjct  100  THRPVNVVNVYNDTQIKLLIKQ--DDDL--EVPAYEDIFRDEEE--DEEHSGNDSDGSEP  153

Query  185  DDEATDADE--VTDEDEEDEDETISNKRGNSS--------------IGP--NDLSKRKQR  226
             ++ T  +E  V       +      + G+ S                GP  +  + R  R
Sbjct  154  SEKRTRLEEEIVEQTMRRRQRREWEARSGSGSEPVAAALEKSSRLFAGPMSDRTAPRSPR  213

Query  227  KKQIHEYEGVLEEYYSQGTTVVNSISAQIYSLLSAIGETNLSN-LWLNILGTTSL---DI  282
            +  + +YE    +Y   GT+     SA +   L+ +   +L++ LW  I+G T     D
Sbjct  214  RDILFDYE----QYEYHGTS-----SAMVMFELAWMLSKDLNDMLWWAIVGLTDQWVQDK  264

Query  283  AYAQVYNRLYPLLQDEVKRLTPSSRNSVKT--PDTLTLNIQPDYYLFLLRHSSLYDSFYY  340
                Y     +LQ  V R    + +   T    D   ++ + D  L L +H SL+DS
Sbjct  265  ITQMKYVTDVGVLQRHVSRHNHRNEDEENTLSVDCTRISFEYDLRLVLYQHWSLHDSLCN  324

Query  341  SNYVNAKLSLWNENGKKRLHKMFARMGIPLSTAQETWLYMDHSIKRELGIIFDKNLDRYG  400
            ++Y  A+  LW+ +G+KRL +  A MG+PL   ++ +  MD S+K  L  + +++ +++G
Sbjct  325  TSYTAARFKLWSVHGQKRLQEFLADMGLPLKQVKQKFQAMDISLKENLREMIEESANKFG  384

Query  401  LQDIIRDGFVRTLGYRGSISASEFVEALTALLEVGNSTDKDSVKINNDNNDDTDGEEEED  460
            ++D+    F    G++    AS+ V A  +L+E   S +KD           TD
Sbjct  385  MKDMRVQTFSIHFGFKHKFLASDVVFATMSLME---SPEKD--------GSGTD------  427

Query  461  NSAQKLTNLRKRWVSNFWLSWDALDDRKVELLNRGIQLAQDLQRAIFNTGVAILEKKLIK  520
                          +F  + D+L    ++ L  G++LA+   RA   T  + L   L+
Sbjct  428  ---------------HFIQALDSLSRSNLDKLYHGLELAKKQLRATQQTIASCLCTNLVI  472

Query  521  HLRIYRLCVLQDG-PDLDLYRNPLTLLRLGNWLIE---CCAESEDKQLLPMVLAS-IDEN  575
               +  C L +G PD+ L+   P +L  L   L++   C  ++   +LLP+V+A+ +
Sbjct  473  SQGPFLYCSLMEGTPDVMLFSRPASLSLLSKHLLKSFVCSTKNRRCKLLPLVMAAPLSME  532

Query  576  TDTYLVAGLTPRYPRGLDTIHTKKPILNNFSMAFQQITAETDAKVRIDNFESSIIEIRRE  635
              T  V G+ P      D+   K    N F  AF++    T +++  ++F+ S+IE++ E
Sbjct  533  HGTVTVVGIPPE----TDSSDRK----NFFGRAFEKAAESTSSRMLHNHFDLSVIELKAE  584

Query  636  DLSPFLEKL  644
            D S FL+ L
Sbjct  585  DRSKFLDAL  593
```

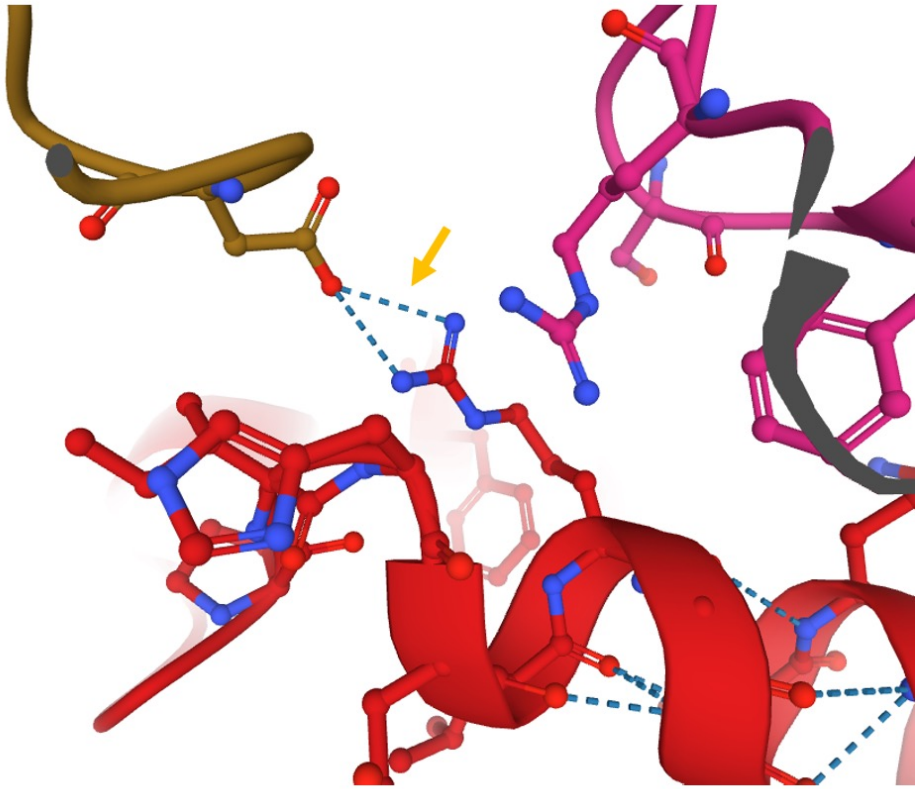

Supplementary figure 2D

```
Query  3    FDRPEIYSAPVLQGESPNDDDN---TEIIKSFKNFILEFRLDSQ-----FIYRDQLRNNI  54
            FD P I+ +    G++  D+     +++ + FK F+ ++R+ +      F YRD+L+ +
Sbjct  4    FDDPGIFYSDSFGGDAQADEGQARKSQLQRRFKEFLRQYRVGTDRTGFTFKYRDELKRHY  63

Query  55   LVKNYSLTVNMEHLIGYNEDIYKKLSDEPSDIIPLFETAITQVAKRISILSRAQSANNND  114
             +  Y + V ME L  ++ED+   L  +P++ + L E A  +VA  ++
Sbjct  64   NLGEYWIEVEMEDLASFDEDLADYLYKQPAEHLQLLEEAAKEVADEVT------------  111

Query  115  KDPENTSMDTDSLLLNSLPTFQLILNSNANQIPLRDLDSEHVSKIVRLSGIIISTSVLSS  174
              P  + +         L   Q++L S+A+   +R L S+ +S +V++ GIII+ S + +
Sbjct  112  -RPRPSGEEV-------LQDIQVMLKSDASPSSIRSLKSDMMSHLVKIPGIIIAASAVRA  163

Query  175  RATYLSIMCRNCRHTTSITINNFNSITG-NTVSLPRSCLSTIESESSMANESNIGDESTK  233
            +AT +SI CR+CR+T    + N     G    +LPR C +               D++ +
Sbjct  164  KATRISIQCRSCRNT----LTNIAMRPGLEGYALPRKCNT---------------DQAGR  204

Query  234  KNCGPDPYIIIHESSKFIDQQFLKLQEIPELVPVGEMPRNLTMTCDRYLTNKVIPGTRVT  293
              C  DPY I+ +  K +D Q LKLQE+P+ VP GEMPR++ + CDRYL +KV+PG RVT
Sbjct  205  PKCPLDPYFIMPDKCKCVDFQTLKLQELPDAVPHGEMPRHMQLYCDRYLCDKVVPGNRVT  264

Query  294  IVGIYSIYnsknqagsgrsgggnggsgVAIRTPYIKILGIQSDVETSSIWNSVTMFTeee  353
            I+GIYSI           +  G    GV IR+ YI++LGIQ D + S   +     + +E
Sbjct  265  IMGIYSI-----KKFGLTTSRGRDRVGVGIRSSYIRVLGIQVDTDGSGR-SFAGAVSPQE  318

Query  354  eeeFLQLSRNPKLYEILTNSIAPSIFGNEDIKKAIVCLLMGGSKKILPDGMRLRGDINVL  413
            EEEF +L+  P +YE+++ SIAPSIFG  D+KKAI CLL GGS+K LPDG+  RGDIN+L
Sbjct  319  EEEFRRLAALPNVYEVISKSIAPSIFGGTDMKKAIACLLFGGSRKRLPDGLTRRGDINLL  378

Query  414  LLGDPGTAKSQLLKFVEKVSPIAVYTSGKGSSAAGLTASVQRDPMTREFYLEGGAMVLAD  473
            +LGDPGTAKSQLLKFVEK SPI VYTSGKGSSAAGLTASV RDP +R F +EGGAMVLAD
Sbjct  379  MLGDPGTAKSQLLKFVEKCSPIGVYTSGKGSSAAGLTASVMRDPSSRNFIMEGGAMVLAD  438

Query  474  GGVVCIDEFDKMRDEDRVAIHEAMEQQTISIAKAGITTVLNSRTSVLAAANPIYGRYDDL  533
            GGVVCIDEFDKMR++DRVAIHEAMEQQTISIAKAGITT LNSR SVLAAAN ++GR+D+
Sbjct  439  GGVVCIDEFDKMREDDRVAIHEAMEQQTISIAKAGITTTLNSRCSVLAAANSVFGRWDET  498

Query  534  KSPGDNIDFQTTILSRFDMIFIVKDDHNEERDISIANHVINIHTGnanamqnqqeenGSE  593
            K   DNIDF  TILSRFDMIFIVKD+HNEERD+ +A HVI +H       Q  +     E
Sbjct  499  KGE-DNIDFMPTILSRFDMIFIVKDEHNEERDVMLAKHVITLHVSALTQTQAVE----GE  553

Query  594  ISIEKMKRYITYCRLKCAPRLSPQAAEKLSSNFVTIRKQLLINELESTERSSIPITIRQL  653
            I + K+K++I YCR+KC PRLS +AAEKL + ++ +R     +E +S  RSSIPIT+RQL
Sbjct  554  IDLAKLKKFIAYCRVKCGPRLSAEAAEKLKNRYIIMRSGARQHERDSDRRSSIPITVRQL  613

Query  654  EAIIRITESLAKLELSPIAQERHVDEAIRLFQASTMDAASQDPIGGLNQASGTSLSE-IR  712
            EAI+RI E+L+K++L P A E  V+EA+RLFQ ST+DAA    + G+    +     E +
Sbjct  614  EAIVRIAEALSKMKLQPFATEADVEEALRLFQVSTLDAALSGTLSGVEGFTSQEDQEMLS  673

Query  713  RFEQELKRRLPIGWSTSYQTLRREFVDTHRFSQLALDKALYALEKHETIQLRHQGQNIYR  772
            R E++LKRR  IG   S  ++ ++F    ++ + A+ K L  + +   IQ R Q + +YR
Sbjct  674  RIEKQLKRRFAIGSQVSEHSIIKDFT-KQKYPEHAIHKVLQLMLRRGEIQHRMQRKVLYR  732
```

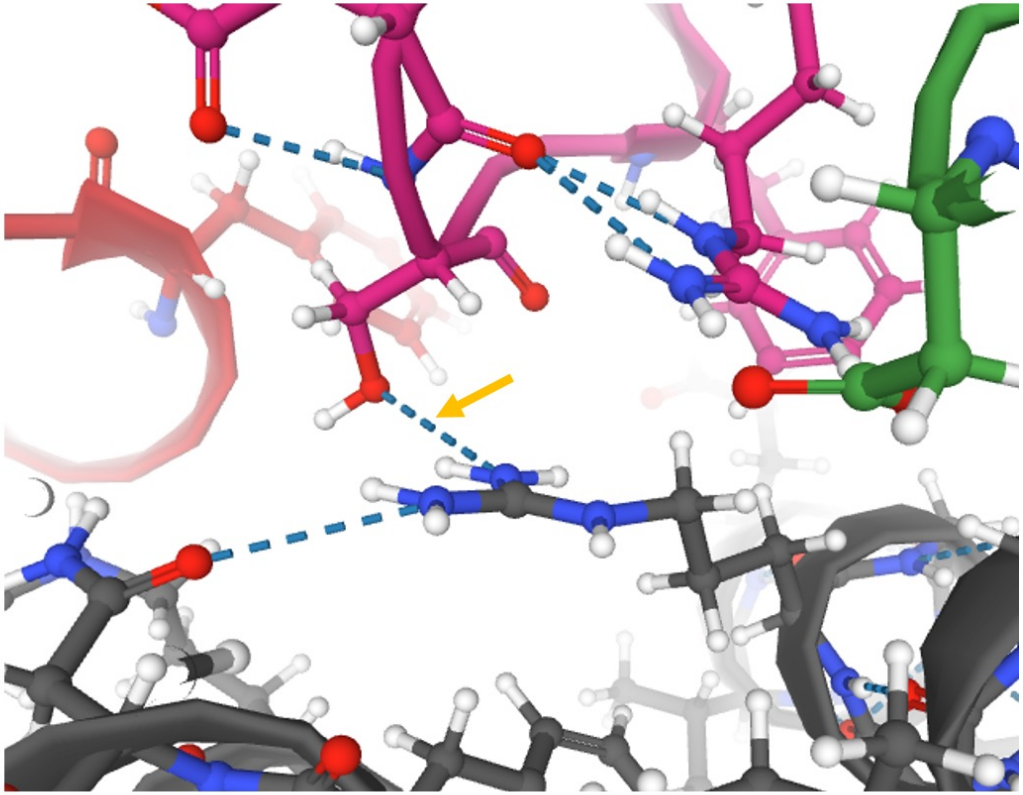

Supplementary figure 2E

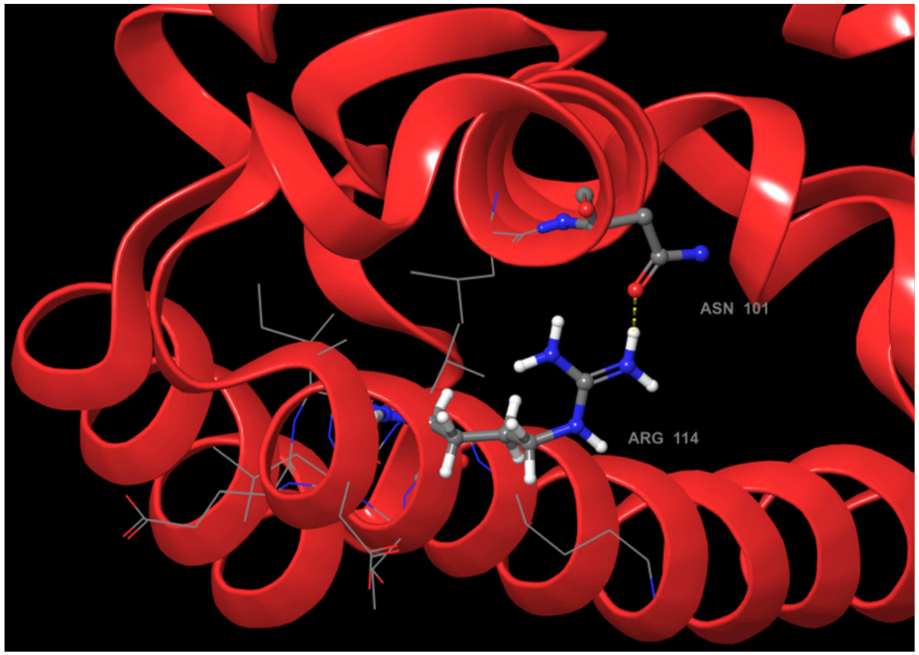

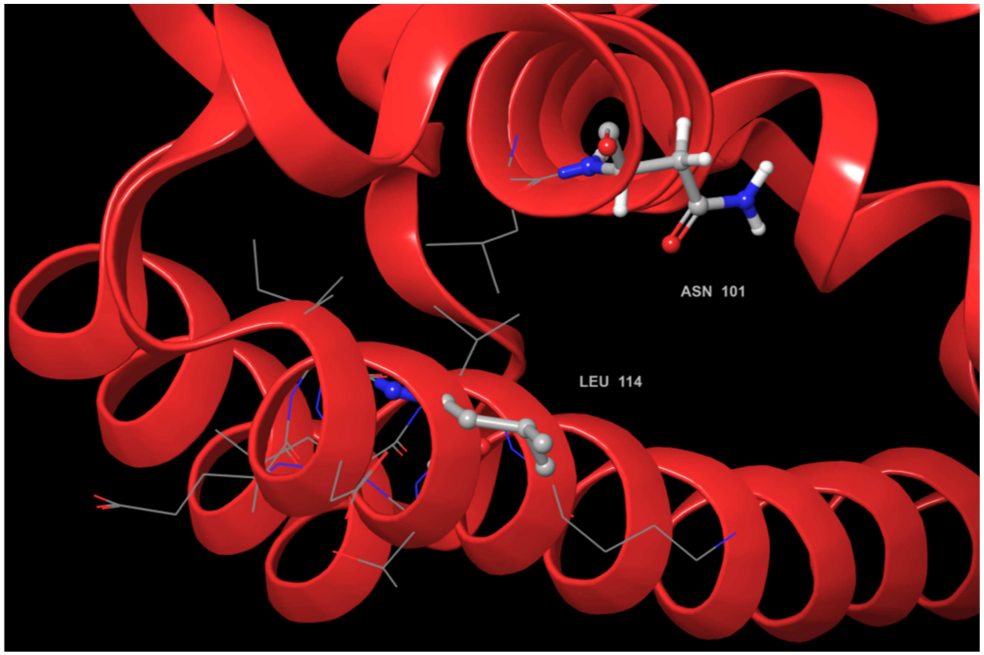

Supplementary figure 2F

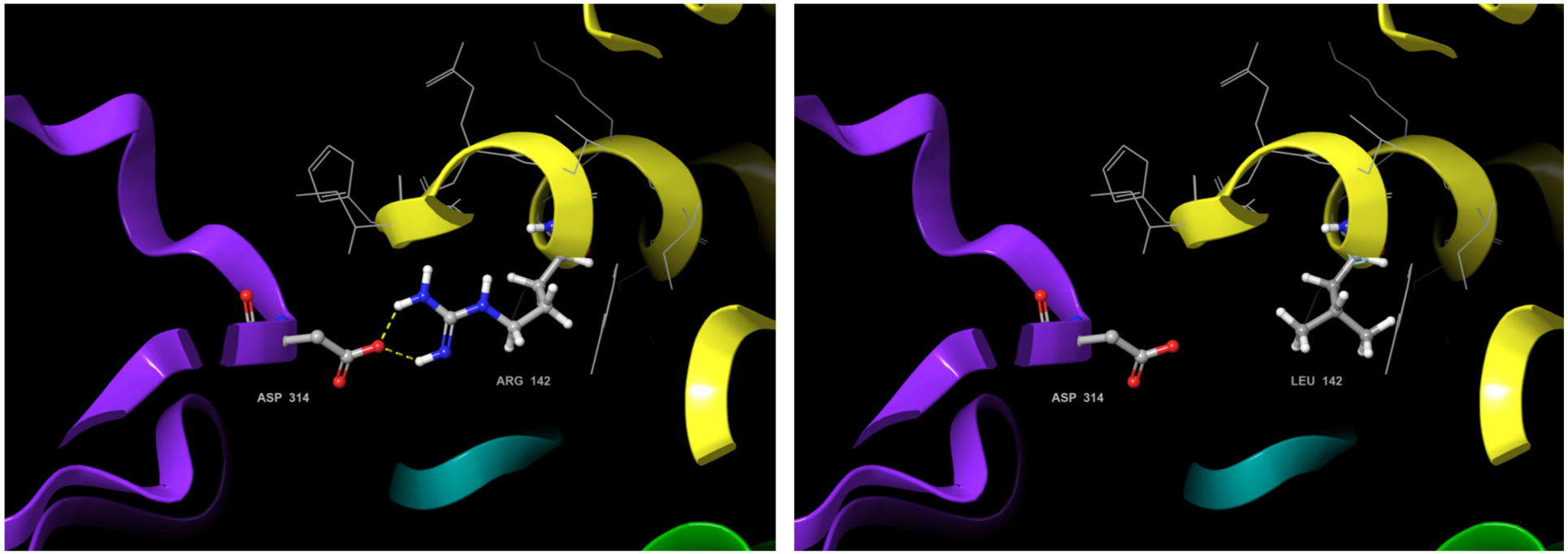

Supplementary figure 2G

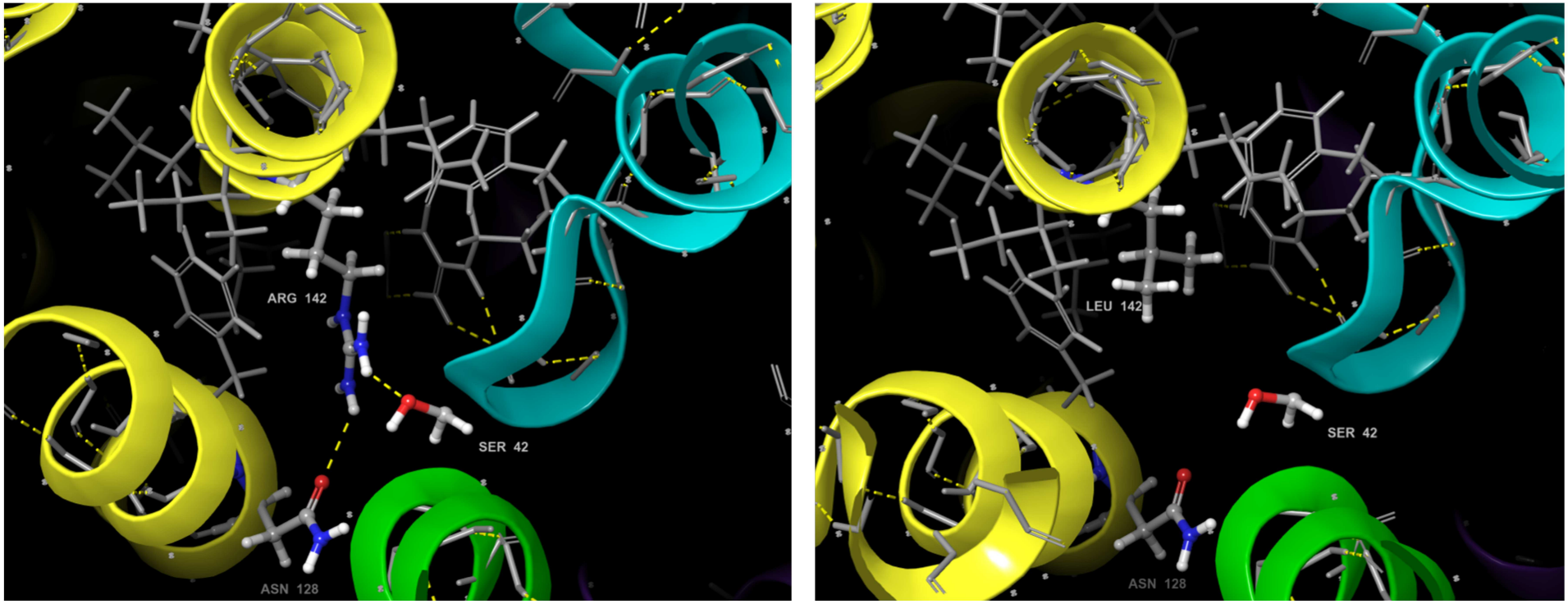

Supplementary table 3. Clinical features of individuals with MGORS or immunodeficiency with genetic defects in components and regulators of the pre-replication and pre-initiation complexes involved in DNA replication

Gene	*GINS2*	*ORC1*	*ORC4*	*ORC6*	*CDT1*	*CDC6*	*GMNN*	*DONSON*	*CDC45*	*MCM5*	*Total*	*MCM4*	*GINS1*
Phenotype	*MGORS*	*MGORS*	*MGORS*	*MGORS*	*MGORS*	*MGORS*	*MGORS*	*MGORS*	*MGORS*	*MGORS*	*MGORS*	*Immuno-deficiency 54*	*Immuno-deficiency 55*
References (PMID)	Present report	21358633, 21358632, 21358631, 11477602	21358632, 21358631, 11477602	21358632, 25691413	21358632, 21358631, 11477602	21358632	26637980	31784481	27374770	28198391		22499342, 18430777, 22354167, 22354170	28414293
N (*number of TOP)*	1 (0)	10 (1)	7 (0)	5 (2)	8 (0)	1 (0)	3 (0)	4 (0)	15 (2)	1 (0)	55 (5)	21 (0)	5 (0)
Gender	F	5M, 5F	1M, 6F	4M, 1F	2M, 6F	M	1M, 2F	3M, 1F	7M, 8F	M	25M, 30F	10M, 11F	1M, 5F
Age at last examination	7y	17w GA - 47y	5y - 23y	20w GA - 15y 5m	4y 4m - 17y 6m	7y	34m - 17y	7y - 29y 10m	22w GA - 28y	4y 8m	17w GA - 47y	0.5y - 17.9y	18m - 29y
Growth													
*Intrauterine growth restriction**	+	+ (8/9)	+ (7/7)	+ (4/4)	+ (7/8)	+ (single case)	+ (2/3)	+ (4/4)	+ (10/15)	+ (single case)	+ (45/53)	+ (19/20)	+ (5/5)
*Short stature***	+	+ (9/9)	+ (6/7)	+ (3/3)	+ (6/8)	+	+ (3/3)	+ (4/4)	+ (10/13)	+	+ (44/50)	+ (18/21)	+ (4/5)
*Microcephaly****	+	+ (8/8)	+ (4/6)	+ (4/4)	+ (3/8)	+	+ (2/3)	+ (3/4)	+ (14/15)	-	+ (40/51)	+ (8/9)	NR
Craniofacial ^													
Microtia / small ears	+	+ (9/10)	+ (7/7)	+ (3/3)	+ (8/8)	+	+ (3/3)	+ (4/4)	+ (13/14)	+	+ (50/52)	NR	NR
Conductive hearing loss	-	+ (1/1)	+ (1/3)	NR	NR	NR	+ (1/3)	+ (2/2)	+ (2/3)	NR	+ (7/13)	NR	NR
Cleft palate	-	- (0/1)	NR	NR	NR	+	+ (1/1)	+ (1/1)	+ (2/2)	NR	+ (5/7)	NR	NR
Microstomia	+	+ (4/6)	+ (4/4)	+ (1/3)	+ (2/7)	-	+ (3/3)	NR	+ (5/8)	+	+ (21/34)	NR	NR
Full lips	+	+ (7/8)	+ (2/4)	+ (3/3)	+ (7/8)	+	+ (3/3)	+ (1/1)	+ (6/7)	+	+ (32/37)	NR	NR
Retro-/micrognathia	+	+ (5/8)	+ (4/4)	+ (5/5)	+ (7/8)	+	+ (3/3)	+ (1/1)	+ (8/8)	+	+ (36/40)	NR	NR
Cardiovascular													
Congenital heart defect	+	NR	+ (1/1)	- (0/1)	+ (1/1)	NR	NR	NR	+ (5/5)	NR	+ (8/9)	+ (1/2)	NR
Respiratory													
Congenital pulmonary emphysema	-	+ (3/4)	+ (1/4)	- (0/4)	+ (4/7)	- (0/1)	+ (1/3)	NR	NR	NR	+ (9/24)	NR	NR

Laryngo-/tracheo-/bronchomalacia	-	+ (1/1)	+ (2/2)	NR	NR	NR	+ (1/3)	NR	NR	NR	+ (4/7)	NR	NR
Gastrointestinal													
Feeding problems	+	+ (3/3)	+ (7/7)	+ (1/2)	+ (3/5)	+	+ (3/3)	NR	NR	-	+ (19/23)	NR	NR
Gastroesophageal reflux	+	+ (2/2)	+ (5/5)	NR	+ (1/1)	+	+ (1/3)	NR	NR	NR	+ (11/13)	+ (1/1)	NR
Mammary glands													
Postpubertal mammary hypo-/aplasia (female)	na	+ (2/2)	+ (5/5)	+ (1/1)	+ (3/3)	na	NR	NR	+ (1/1)	na	+ (12/12)	NR	NR
Genitourinary ┬													
Hypoplastic labia minora/majora (female)	NR	NR	+ (3/3)	NR	+ (1/1)	na	+ (1/1)	NR	NR	na	+ (5/5)	NR	NR
Micropenis (male)	na	+ (1/3)	NR	+ (1/3)	- (0/2)	+	NR	NR	+ (1/1)	NR	+ (4/10)	NR	NR
Cryptorchidism (male)	na	+ (2/3)	NR	+ (2/2)	+ (1/2)	+	+ (1/1)	NR	+ (1/1)	+	+ (9/11)	NR	NR
Skeletal													
Craniosynostosis	+	+ (1/1)	NR	NR	NR	NR	NR	NR	+ (12/13)	NR	+ (14/15)	NR	NR
Delayed bone age	+	+ (3/3)	+ (1/3)	+ (2/3)	+ (3/4)	+	+ (2/2)	+ (1/1)	NR	NR	+ (14/18)	+ (5/5)	NR
Patellar aplasia/hypoplasia	+	+ (4/7)	+ (7/7)	+ (4/4)	+ (8/8)	+	+ (3/3)	+ (4/4)	+ (8/11)	+	+ (41/47)	NR	NR
Neurologic													
Development delay / Intellectual disability	-	+ (2/8)	- (0/7)	- (0/3)	- (0/8)	-	+ (2/3)	+ (3/4)	+ (3/12)	-	+ (10/48)	+ (5/6)	NR
Immunologic													
Recurrent infections	+	+ (1/1)	NR	NR	+ (1/1)	NR	NR	NR	NR	+	+ (4/4)	+ (9/16)	+ (5/5)
NK cell deficiency	-	NR	NR	NR	NR	NR	NR	NR	NR	-	- (0/2)	+ (16/16)	+ (5/5)
Neutropenia	-	NR	NR	NR	NR	NR	NR	NR	NR	-	- (0/2)	+ (3/3)	+ (5/5)
Endocrinologic													
Adrenal insufficiency	NR	NR	NR	NR	NR	NR	NR	NR	NR	NR	NR	+ (20/21)	NR

na, not applicable. NR, not reported. M, male. F, female. m, months. Y, years-old. GA, gestational age. w, weeks *Abnormal restriction of fetal growth with fetal weight below the tenth percentile for gestational age. **Height more than 2 standard deviations below the mean for age and gender. ***Head circumference more than 2 standard deviations below the mean for age and gender. ^Thin eyebrows were reported in all 15 individuals with biallelic *CDC45* variants. ⊤Anal abnormalities were reported in 7/7 individuals with biallelic *CDC45* variants. NB. This case series review was based on the data of 80 individuals previously reported in the literature. In retrospective studies, which rely on data from existing records and mostly not collected for research purposes, clinical information may be missing (e.g. individuals may have developed a feature that was not reported, or they may still be at risk and not have developed the clinical feature at the time of the study). Thus, "Attention should be paid to the missing data in the analysis of the resulting data, as missing data can reduce the representativeness of the samples and can produce biased estimates, leading to invalid conclusions (PMID 23741561; PMID 32847800)." A detailed molecular and clinical characterization of each individual included in this review is available in Supplementary table 3.

Supplementary Table 5. Genotypes of yeast strains used in this study.

Strain	Genotype	Reference
BY4743	BY4743 *MAT a/alpha his3Δ1/his3Δ1 leu2Δ0/leu2Δ0 LYS2/lys2Δ0 met15Δ0/MET15 ura3Δ0/ura3Δ0*	PMID: 9483801.
BY4741	BY4741 *MAT a his3Δ1/his3Δ1 leu2Δ0/leu2Δ0 ura3Δ0/ura3Δ0*	PMID: 9483801.
MMY5811	BY4741 *PSF2-WT::kanMX*	This study
MMY5815	BY4741 *psf2-R142L::kanMX*	This study

Reference:

Brachmann CB, Davies A, Cost GJ, Caputo E, Li J, Hieter P, Boeke JD. Designer deletion strains derived from *Saccharomyces cerevisiae* S288C: A useful set of strains and plasmids for PCR-mediated gene disruption and other applications. *Yeast* 1998;14:115-132. PMID: 9483801.

Supplementary Table 6. Oligonucleotide primers used in this study.

Primer	Sequence
p416-PSF2_Fwd	CTCACTAAAGGGAACAAAAGCTGGAGCTCAGTTTATCTCTTTATGACACTTGAAAAC
p416-PSF2_Rev	CAAGGCGATTAAGTTGGGTAACGCCAGGGTTTTCCCAACAACAACAGCAGCAACAAC
PSF2-R142L_Fwd	CCCATTCACGAATTACTTGGTAAAATACAAGAC
PSF2-R142L_Rev	GTCTTGTATTTTACCAAGTAATTCGTGAATGGG
PSF2-C	TTTAAATAATATGGTAGCCATGCGT
PSF2-D	ACCATAACGACAAACAAGAATCAAT
PSF2-F2-STOP	CACAGCATCTCTTACCGCTGGTACTGAAAATGATGAAGAAGAATTCAATATTTAACGGATCCCCGGGTTAATTAA
PSF2-R1	ATATATACATACGCATATCACTGAAAGTTCTAATTATTGCAAAGCCAGCACTTTTGAATTCGAGCTCGTTTAAAC